Analysis of the Solvent- and Temperature-Dependent Raman Spectral Changes of S_1 *trans*-Stilbene and the Mechanism of the trans to cis Isomerization: Dynamic Polarization Model of Vibrational Dephasing and the C═C Double-Bond Rotation†

Koichi Iwata, Ryosuke Ozawa, and Hiro-o Hamaguchi*

Research Centre for Spectrochemistry and Department of Chemistry, School of Science, The University of Tokyo, 7-3-1 Hongo, Bunkyo-ku, Tokyo 113-0033, Japan

Received: August 30, 2001; In Final Form: December 6, 2001

Solvent- and temperature-dependent band shape changes of the olefinic C═C stretch Raman band of S_1 *trans*-stilbene have been analyzed on the basis of the dynamic polarization model. The analysis has shown that the solvent-induced dynamic polarization gives rise to the dephasing of the C═C stretch vibration and, concomitantly, triggers and facilitates the rotation around the C═C bond leading to the trans to perpendicular (and eventually to cis) isomerization. Picosecond time-resolved Raman spectra have been measured in the three alkane solvents, hexane, octane, and decane at a number of different temperatures ranging from 268 to 338 K and a total of 40 peak positions and the bandwidths have been determined for the C═C stretch band. The correlation plot of the bandwidth against peak position shows a clear linear relationship that is predicted by the dynamic polarization model. Picosecond time-resolved fluorescence measurements have been performed in the same three alkane solvents at five different temperatures from 283 to 313 K, and 15 rates of the trans to perpendicular isomerization have been determined. The plot of the peak position against the rate of isomerization indicates another linear relationship between these two quantities which have no obvious reason to be correlated with each other. The dynamic polarization model accounts very well for this linear relationship and yields a new formula that relates the rate of isomerization to the frequency of the solvent-induced dynamic polarization. This formula seems to possess certain generality because it shows an excellent numerical agreement with the Arrhenius formula. The new formula derived from the dynamic polarization model gives the molecular-level details of the reaction process as to how the reaction is triggered and in what time scale the reaction actually proceeds. A new view of the photoisomerization of *trans*-stilbene has thus been obtained.

Introduction

Vibrational Raman band shapes carry useful information on vibrational dynamics of molecules in liquids and solutions. Numerous experimental and theoretical studies have been carried out on Raman band shapes of molecules in their ground electronic states.[1] Separate measurements of the isotropic and anisotropic components of polarized Raman spectra enable the differentiation of the Raman bandwidth caused by rotational diffusion and that caused by vibrational dephasing. Rotational diffusion times of a number of molecules in liquids and solutions have thus been determined by Raman spectroscopy. On the other hand, information extracted from vibrational dephasing times varies depending on the type of intermolecular interaction that predominates the dephasing process. Development of time-resolved Raman spectroscopy in the past decade has made it possible to extend those band shape studies to electronically excited states and radical species.[2,3] Raman bandwidths of these short-lived species are generally much larger than those of the corresponding ground-state molecules. Because rotational diffusion makes only a minor contribution to Raman bandwidths of medium to large size polyatomic molecules and because they are expected to be similar for the ground and excited electronic states, the observed larger bandwidths are most probably due to shorter vibrational dephasing times. It is considered that some extra vibrational dephasing mechanism exists which is specific to excited states and radical species.

Raman spectra of S_1 *trans*-stilbene have been studied extensively since the first observation in 1983.[4−43] Marked time-, temperature-, and solvent-dependent Raman band shape changes are known for the olefinic C═C stretch band observed around 1570 cm^{-1}. The central issue in these studies is how these spectral changes are elucidated to shed more light on the mechanism of the trans to cis isomerization reaction, which has been studied thoroughly as one of the simplest prototype of chemical reactions.[44,45] It is already established that the S_1 *trans*-stilbene molecule first isomerizes to the 90° twisted perpendicular form and then very quickly transforms to either of the trans and cis forms with nearly a 50:50 ratio. The rate of the overall trans to cis isomerization is determined by the rate of the trans to perpendicular conversion.

From a comparison with the Stokes/anti-Stokes Raman intensity ratio, it has been proved that the time-dependent change represents the cooling process of the hot S_1 *trans*-stilbene molecule that is generated with extra vibrational energy upon photoexcitation.[29,33] The time-dependent band shape changes have the same origin as the temperature-dependent changes. Picosecond time-resolved Raman spectroscopy can serve as "picosecond thermometry" that probes the temperature of the S_1 *trans*-stilbene system with picosecond time resolution. The temperature- and solvent-dependent band shape changes possess

† Part of the special issue "Mitsuo Tasumi Festschrift".

* To whom correspondence should be addressed. Fax: +81-3-3818-4621. E-mail: hhama@chem.s.u-tokyo.ac.jp.

10.1021/jp013359y CCC: $22.00
Published on Web 03/19/2002

a characteristic feature in common. The shift of the peak position and the change in the bandwidth are linearly correlated with each other,[20,32] though there is no intrinsic reason why they should be correlated. If we plot the observed peak position against the bandwidth for different temperatures and solvents, we obtain nice straight lines. This finding led the present authors to introduce the exchange model[20] (generalized later as the dynamic polarization model[46]) of vibrational dephasing, which accounted very well for this linear relationship between the peak position and the bandwidth. A still more interesting and somewhat surprising feature has been discovered for the solvent-dependent Raman band shape changes; the shift of the peak position and the change in the bandwidth are correlated linearly with the (solvent-dependent) rate of the trans to the perpendicular isomerization.[44,45] This correlation has also been explained well in terms of the exchange model.

In the present paper, we examine in further details the solvent- and temperature-dependent Raman spectral changes of S_1 *trans*-stilbene from a unified viewpoint of the dynamic polarization model, which is a generalized version of the exchange model. Picosecond time-resolved Raman spectra were measured in three different alkane solvents, hexane, octane, and decane, at more than 10 different temperatures, and a total of 40 peak positions and bandwidths have been determined for the olefinic C═C stretch band. The correlation plot of the 40 peak positions and bandwidths confirms beyond any doubt the linear relationship between these two quantities, rationalizing further analysis based on the dynamic polarization model. Fluorescence lifetimes were measured in the same three solvents at five different temperatures, and 15 isomerization rates have been determined. The five iso-temperature plots of the peak position against the isomerization rate give five straight lines having slopes gradually changing with temperature and having a common intercept at zero isomerization limit. These two correlations, the correlation between the peak position and the bandwidth of the olefinic C═C stretch mode and the correlation between the peak position and the isomerization rate, are difficult to explain quantitatively with any existing theory of vibrational dephasing. For example, the temperature-dependent changes of the peak position and bandwidth may be explainable in terms of a hot band mechanism which assumes the excitation of some low-frequency vibrational mode(s) anharmonically coupled to the C═C mode. However, this model cannot account for the solvent-dependent changes of the peak position and the bandwidth and their correlation with the isomerization rate. These two correlations are discussed quantitatively in the following on the basis of the dynamic polarization model.

Experimental Section

Picosecond time-resolved Raman spectra were measured with the pump−probe technique. The details of the experimental setup have already been published.[47] Output pulses from a cw mode-locked Nd:YAG laser (Spectra Physics 3800S, 82 MHz) were compressed with a glass fiber and a grating. The compressed pulses (5 ps) were used for exciting a synchronously pumped mode-locked dye laser (Spectra Physics 3520). The dye laser output was then amplified with a two-stage dye amplifier. Output from a cw Nd:YAG regenerative amplifier (2 kHz) was used for the dye amplification. The second harmonic of the amplifier output (294 nm, 2 kHz, 2−3 mW) was used as the pump light source. The remaining visible light (588 nm, 2 kHz) was used as the probe. The temporal width of the probe light pulse was 3.2 ps while its spectral width was 3.5 cm^{-1}. The light pulse was close to the Fourier transform limit.[47] Time delay between the pump and probe pulses were regulated by a stepping-motor driven optical delay line. We reduced the probe light power at the sampling point to 0.1 mW for avoiding deformation of the shapes and positions of observed Raman bands, caused by strong probe light field. Scattered light from the sample was collected by a pair of lenses, was focused into the entrance slit of a single polychromator (Instruments SA, HR320), and was detected with a liquid-nitrogen-cooled CCD detector (Princeton Instruments LN/CCD-1024 TKB).

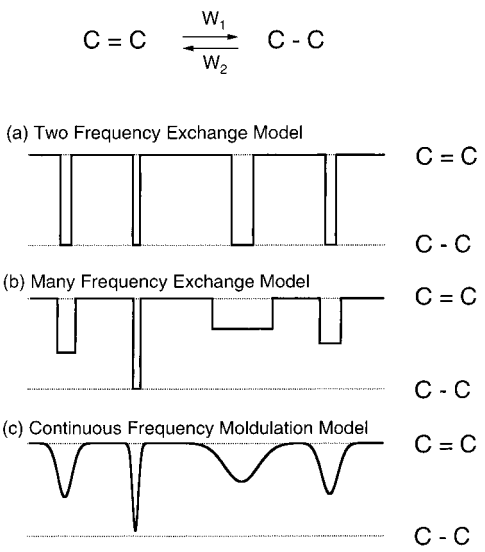

Figure 1. Three models for stochastic modulation of vibrational frequencies assumed in the dynamic polarization model. Two-frequency exchange model (a), many-frequency exchange model (b), and continuous-frequency modulation model (c).

Picosecond time-resolved fluorescence spectra were measured with an apparatus that consisted of a mode-locked Ti:sapphire laser system and a streak camera.[48] Output from a cw mode-locked Ti:sapphire laser (80 MHz, laboratory-made) pumped by an argon ion laser (Spectra Physics BeamLok 2060) was amplified with a Ti:sapphire regenerative amplifier (Clark Instruments CPA-1). Third harmonic of the amplifier output (266 nm, 1 kHz, 2 mW) was used for the sample excitation. The fluorescence component with a 54.7° polarization angle to the excitation polarization was collected with lenses and then analyzed with an astigmatism corrected spectrograph (Chromex 500IS/SM) and was detected with a streak camera (Hamamatsu C2909, modified). Remaining fundamental output from the regenerative amplifier was used for triggering the streak camera. Time resolution of the apparatus was determined by a timing jitter of the streak camera. Typical width (fwhm) of the instrumental response function was 15 ps.

Dynamic Polarization Model

In a previous paper, we formulated the dynamic polarization model of vibrational dephasing in three steps.[46] Figure 1 schematically shows how the stochastic modulation of the vibrational frequency of the C═C stretch mode is treated in the three models: the two-frequency exchange model, the distributed frequency exchange model, and the continuous dynamic polarization model. We started with the two-frequency exchange model (Figure 1a) in which the vibrational frequency hops to and fro between the two limiting values ω_1 and ω_2 with the frequency difference $\delta\omega = \omega_2 - \omega_1$. In the case of S_1 *trans*-stilbene, ω_1 corresponds to the C═C double-bond frequency and ω_2 to the fully polarized C−C (C^+-C^- or $\dot{C}-\dot{C}$) single-bond frequency. For this simple case, a general formula of the

band shape was already known.[49,50] We placed a focus on the asymmetric exchange limit, in which the frequency stays most of the time at ω_1 and occasionally hops to ω_2 (with the forward hopping rate W_1) but comes back to ω_1 very quickly (with the backward hopping rate of W_2), so that $W_1 \ll W_2 \sim \delta\omega$ holds. Under these conditions, the band shape is given by a Lorentzian with a small shift $\Delta\Omega$ of the peak position and a small increase $\Delta\Gamma$ in the bandwidth from the original unperturbed Lorentzian band shape,

$$\Delta\Omega = W_1\tau/(1+\tau^2) \tag{1}$$

$$\Delta\Gamma = W_1\tau^2/(1+\tau^2) \tag{2}$$

where $\tau = \delta\omega/W_2$ is the mean phase shift for a hop. In the simple two-frequency exchange model, the band shape is determined by the two parameters, the forward hopping rate W_1 and the mean phase shift τ. If we take the ratio of $\Delta\Gamma$ to $\Delta\Omega$, we obtain the following formula:

$$\Delta\Gamma/\Delta\Omega = \tau \tag{3}$$

This equation indicates that, if the mean phase shift τ can be regarded as constant for different solvents and temperatures, the band shape does change holding a linear correlation between the peak position Ω and the bandwidth Γ. Thus, the experimental linear relationship between Ω and Γ is very well accounted for by the two-frequency exchange model.

We then considered the distributed-frequency exchange model (Figure 1b) in which the vibrational frequency can take n values including the limiting frequencies ω_1 and ω_n. In the case of S_1 *trans*-stilbene, ω_1 corresponds to the C═C frequency and ω_n to the C−C frequency, with ω_k ($1 < k < n$) standing for any intermediate frequencies. By assuming that a hop always starts from ω_1 and that each hop is independent, we obtain formulas corresponding to eqs 1 and 2:

$$\Delta\Omega = W_1\sum_{\kappa=2}^{n}(W_{1\kappa}/W_1)\tau_\kappa/(1+\tau_\kappa{}^2) \tag{4}$$

$$\Delta\Gamma = W_1\sum_{\kappa=2}^{n}(W_{1\kappa}/W_1)\tau_\kappa{}^2/(1+\tau_\kappa{}^2) \tag{5}$$

where W_{1k} is the partial forward hopping rate from ω_1 to ω_k ($W_1 = \sum W_{1k}$) and τ_κ is the mean phase shift for a hop to ω_n. Equations 4 and 5 mean that the hops to different frequencies make independent contributions to the vibrational band shape and that each contribution is described by the same formulas as eqs 1 and 2. If we assume that all of the mean phase shifts τ_κ are constant and are equal to τ, eqs 4 and 5 reduce to eqs 1 and 2. This condition is equivalent to the relation $W_{k1} = \delta\omega_k/\tau$, where W_{k1} is the backward hopping rate from ω_k to ω_1 and $\delta\omega_k = \omega_k - \omega_1$. It seems physically sound that the backward hopping rate W_{k1} is, to a first-order approximation, proportional to the frequency change $\delta\omega$, because the solvent fluctuation causing a larger frequency hop is likely to have a shorter duration. Thus, relationships in eqs 1−3 hold approximately for the distributed frequency exchange model.

Although the exchange models provided simple formulas with clear physical meanings, they assumed instantaneous jumps of frequencies which were not likely to happen in the real system. We therefore proceeded to the dynamic polarization model (Figure 1c) in which the vibrational frequency is continuously modulated by the solvent fluctuation. For this model, the mathematical approach used for the exchange models is not applicable. However, considering the fact that each hop contributes to the band shape only through the phase shift τ as eqs 4 and 5 indicate, we proposed the following two integral formulas which are expected to hold for the continuous frequency modulation case:

$$\Delta\Omega = \frac{W_1\int_{-\infty}^{0} G(\tau)\tau/(1+\tau^2)\,\mathrm{d}\tau}{\int_{-\infty}^{0} G(\tau)\,\mathrm{d}\tau} \tag{6}$$

$$\Delta\Gamma = \frac{W_1\int_{-\infty}^{0} G(\tau)\tau^2/(1+\tau^2)\,\mathrm{d}\tau}{\int_{-\infty}^{0} G(\tau)\,\mathrm{d}\tau} \tag{7}$$

where $G(\tau)$ is the phase shift distribution function which gives the magnitude and frequency of the phase shifts induced by the solvent fluctuation. The phase shift distribution function $G(\tau)$ varies, in general, with solvent and temperature. If, however, $G(\tau)$ can be regarded as the same for some like solvents and for a certain range of temperature, eqs 6 and 7 indicate that $\Delta\Omega$ and $\Delta\Gamma$ are both proportional to W_1 and that a linear relationship holds between the peak position Ω and the bandwidth Γ.

To obtain an expression corresponding to eq 3, we assumed a Gaussian distribution of the phase shift, $G(\tau) = \exp(-\ln 2\tau^2/\tau_{1/2}{}^2)$, where $\tau_{1/2}$ is the half width of the Gaussian. A numerical calculation then showed that for small $\tau_{1/2}$ ($\tau_{1/2} < 0.5$) we have a simple approximate relation between the $\Delta\Gamma$ and $\Delta\Omega$:

$$\Delta\Gamma/\Delta\Omega = \tau_{1/2} \tag{8}$$

This equation has the same form as eq 3 except that the mean phase shift τ in the two-frequency exchange model is replaced by the half width $\tau_{1/2}$ of the phase shift distribution function $G(\tau)$. A linear relationship between $\Delta\Gamma$ and $\Delta\Omega$ has thus been obtained also from the dynamic polarization model.

Results and Discussion

Temperature-Dependent Band Shape Changes of the C═C Stretch Band. Picosecond time-resolved Raman spectra of the S_1 state of *trans*-stilbene were measured at various temperatures in hexane, octane, and decane. For all of the measurements, sample solutions were excited with the pump light of 294 nm. Resonance Raman spectra of generated S_1 *trans*-stilbene were recorded with the probe light of 588 nm. Time delay between the pump and probe pulses was set to be 50 ps. Because the time dependent change of the peak position and the bandwidth is complete by 50 ps after the photoexcitation,[17,18] the observed Raman bands are not affected by these time-dependent changes. Typical examples of the obtained spectra are presented in Figure 2, where spectra measured at 274.2 K (a), 283.8 K (b), 293.3 K (c), 303.6 K (d), and 322.8 K (e) in octane are shown. Although we observe several intense Raman bands from S_1 *trans*-stilbene in the fingerprint region, only the spectral region between 1500 and 1650 cm^{-1}, where the olefinic C═C stretch band is observed, is shown in the figure. It is obvious that the peak position of the observed Raman bands moves to the lower wavenumber direction as the temperature is increased with concomitant increase in the bandwidth.

Because the photon energy of the probe light at 294 nm is larger than the 0−0 transition energy between the S_1 and S_0 states of *trans*-stilbene, vibrational excess energy of ap-

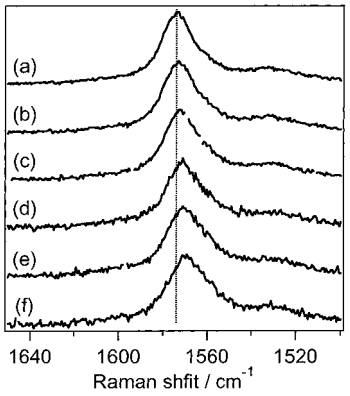

Figure 2. Temperature dependence of the observed olefinic C═C stretch Raman bands of S_1 *trans*-stilbene in octane. Each spectrum was measured at 274.2 (a), 283.8 (b), 293.3 (c), 303.6 (d), and 322.8 K (e).

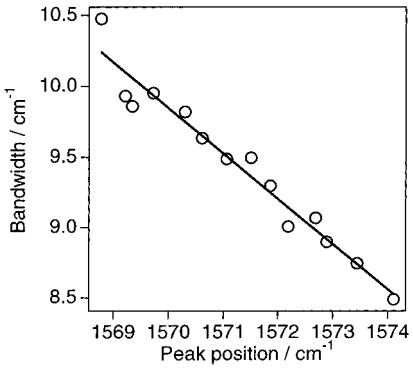

Figure 3. Relationship between the bandwidth and the peak position of the olefinic C═C stretch Raman band of S_1 *trans*-stilbene in octane. Each data point represents one of 14 different temperatures between 268 and 322 K. The result of the least squares calculation (slope, -0.32 ± 0.02) is shown with solid line.

proximately 3000 cm^{-1} is deposited to S_1 *trans*-stilbene upon the photoexcitation. Our "picosecond Raman thermometry" experiment, however, has revealed that S_1 *trans*-stilbene cools with a time constant of 10∼20 ps.[29,33] Therefore, we can safely assume that the excess energy of S_1 *trans*-stilbene has been already dissipated to the bulk solvent at 50 ps when the measurements are performed. In our experimental conditions, S_1 *trans*-stilbene and the surrounding solvent molecules are in equilibrium at given temperatures.

The peak positions and bandwidths of the observed Raman bands were obtained by fitting Lorentzian functions to their symmetric portion. Note that the lower wavenumber side of the olefinic C═C stretch band is affected by the nearby ring C═C stretch band around 1530 cm^{-1}. Data from three different sets of experiments were averaged for determining the final bandwidth and the peak position values. In Figure 3, the bandwidths Ω thus obtained are plotted against the peak positions Γ for octane. The 14 data points represent 14 different temperatures from 268 to 332 K. There is a clear linear relationship between Ω and Γ. The best fitted line obtained from a least-squares analysis is also shown in Figure 3. The slope gives the relation $\Delta\Gamma/\Delta\Omega = -0.32 \pm 0.02$. As already pointed out in previous papers,[20,32] there is no apparent reason why we should expect a linear relationship between the bandwidths and the peak positions of observed Raman bands. A linear correlation similar to the present observation has been reported for time-dependent spectral change of this Raman band in hexane.[20]

Solvent-Dependent Band Shape Change of the C═C Stretch Band. The peak position and the bandwidth of the olefinic C═C stretch Raman band obtained at a particular

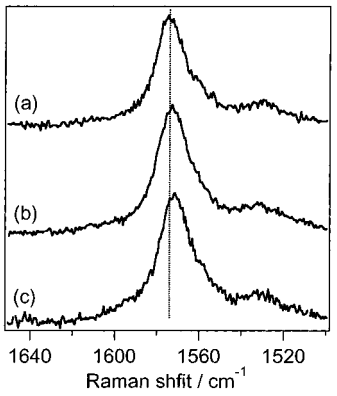

Figure 4. Solvent dependence of the observed olefinic C═C stretch Raman bands of S_1 *trans*-stilbene. Each spectrum was measured in decane at 282.9 K (a), in octane at 283.8 K (b), and in hexane at 283.9 K.

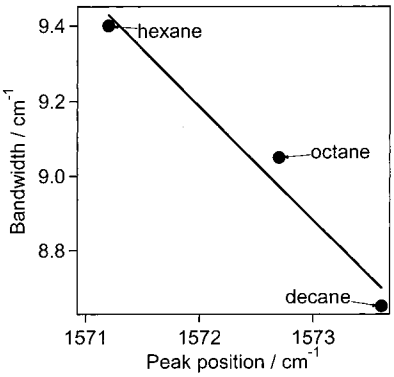

Figure 5. Relationship between the bandwidth and the peak position of the olefinic C═C stretch Raman band of S_1 *trans*-stilbene in three alkane solutions at 283 K. The result of the least squares calculation (slope, -0.30 ± 0.06) is shown with solid line.

temperature change depending on the solvent. Figure 4 shows the observed band shapes for decane (a), octane (b), and hexane (c) at 283 ± 1 K. The peak position shifts to the lower wavenumber direction as the solvent is changed from decane to hexane, and the bandwidth increases concomitantly. The peak position Ω and the bandwidth Γ of each Raman band have been obtained once again by the same analysis as used in the previous section. The results for 283 K are plotted in Figure 5. Although there are only three points in the plot, these points form a good straight line, which is also shown in the figure. The slope gives $\Delta\Gamma/\Delta\Omega = -0.30 \pm 0.06$.

Correlation between the Peak Position and the Bandwidth of the C═C Stretch Band. To examine the solvent- and temperature-dependent spectral changes from a unified viewpoint, we plot in Figure 6 a total of 40 pairs of the observed peak positions and bandwidths for different solvents and temperatures. The plot shows convincingly that a linear relationship holds between the peak position Ω and the bandwidth Γ in the three like solvents and in the temperature range of 268∼338 K. It is noticed that the data points at lower peak positions/larger bandwidths scatter more compared with those at higher peak positions/smaller bandwidths. This tendency is explained by the fact that those data points at lower peak positions/larger bandwidths have been obtained from the lower S/N Raman spectra which were measured with smaller population of the S_1 state. Note that the time-resolved Raman measurements were carried at the fixed delay time of 50 ps and that the S_1 lifetime was not much longer than 50 ps for hexane and octane at high temperatures. By a least-squares fitting of all of the data points to a straight line (shown as a solid line in

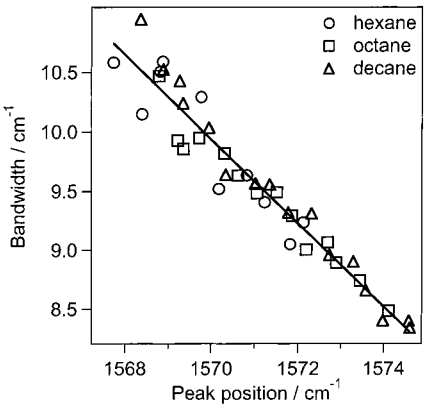

Figure 6. Relationship between the bandwidth and the peak position of the olefinic C═C stretch Raman band of S_1 *trans*-stilbene in three alkane solutions of hexane, octane, and decane. Each data point represents one of 40 different combinations of solvent and temperature. The temperature ranges from 268 to 338 K. The result of the least squares calculation for all the data points (slope, -0.35 ± 0.01) is shown with solid line.

Figure 6), we obtain from the slope $\Delta\Gamma/\Delta\Omega = -0.35 \pm 0.01$. This value corresponds well to the value for the temperature-dependent changes, $\Delta\Gamma/\Delta\Omega = -0.32 \pm 0.02$ and to that for the solvent-dependent changes, $\Delta\Gamma/\Delta\Omega = -0.30 \pm 0.06$. It also agrees with our previous results, $\Delta\Gamma/\Delta\Omega = -0.31$ for S_1 *trans*-stilbene[20] and $\Delta\Gamma/\Delta\Omega = -0.36$ for S_1 *trans*-stilbene-d_5.[32]

The results shown in Figure 6 are fully consistent with eq 8, rationalizing further discussion on the basis of the dynamic polarization model. From eqs 6 and 7, we consider that vibrational dephasing of the C═C stretch mode in hexane, octane, and decane in the temperature range of 268∼338 K is characterized by one common Gaussian phase shift distribution function having a half width of $\tau_{1/2} = -0.35$. Then, the C═C band shape is a function of the forward hopping rate W_1 only. As is shown in the following, W_1 increases with increasing the solvent mobility (decane < octane < hexane), and in accordance with this trend, the observed peak position is higher, whereas the bandwidth is smaller in the order of decane > octane > hexane. With increasing temperature, W_1 increases, giving rise to a shift of the peak position to a lower frequency and a concomitant increase in the bandwidth. Thus, we have explained qualitatively the solvent- and temperature-dependent band shape changes of the C═C stretch mode of S_1 *trans*-stilbene from a unified viewpoint on the basis of the dynamic polarization model. A more quantitative discussion on W_1 is given in the following.

In the framework of the two-frequency exchange model, eq 3 indicates that $\tau = \delta\omega/W_2 = -0.35$. Then, the backward hopping rate W_2 is also constant in the three like solvents and in the temperature range of 268∼338 K, because the frequency difference $\delta\omega$ is most probably independent of the solvent and temperature. If we assume $\delta\omega = 200$ cm^{-1} (3.8×10^{13} rad s^{-1}), we have $W_2 = 1.1 \times 10^{14}$ s^{-1} meaning that the average duration of the solvent fluctuation causing the C═C frequency hop is about 10 fs. If $\delta\omega = 100$ cm^{-1}, $W_2 = 5.4 \times 10^{13}$ s^{-1}, and the average duration of the fluctuation becomes about 20 fs. In the dynamic polarization model, we can discuss only semiquantitatively that the average frequency change of a few hundred wavenumbers and the average duration of a few tens of femtoseconds are consistent with the experimental results.

Correlation between the Peak Position and the Rate of Isomerization. We now discuss the correlation of the peak position and the rate of the trans to perpendicular isomerization.

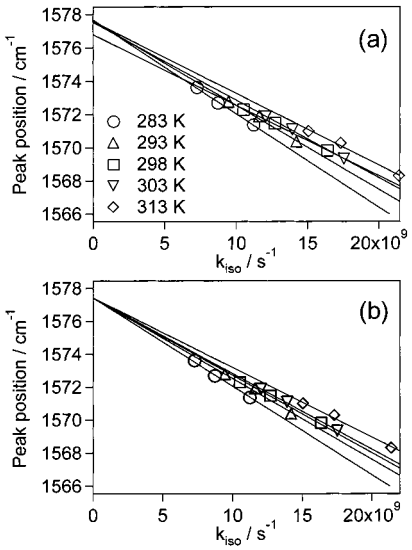

Figure 7. Peak positions of the olefinic C═C stretch Raman band of S_1 *trans*-stilbene in three alkane solutions of hexane, octane, and decane plotted against trans to perpendicular isomerization rate. The peak positions and the isomerization rates were measured at temperatures shown in the figure. The result of least-squares analysis, assuming five linear functions corresponding to five temperatures, is shown in a with five solid lines. The result of least-squares analysis with five linear functions with a common intercept is shown in b.

TABLE 1: Slopes and Intercept for the Observed Peak Position of the Olefinic C═C Stretch Raman Band (Ω) and Observed trans−perpendicular Isomerization Rate (k_{iso}) of S_1 *trans*-stilbene for Five Temperatures, Obtained from a Least Squares Analysis[a]

T/K	Ω/k_{iso}/ cm^{-1} s	W_1/k_{iso}[b]	$10^3P(T)$[c]	ln $P(T)$	$\Delta E'$[d]/ kcal mol^{-1}
283	-5.37×10^{-10}	480	2.1	−6.2	3.5
293	-4.90×10^{-10}	440	2.3	−6.1	3.5
298	-4.70×10^{-10}	420	2.4	−6.0	3.6
303	-4.60×10^{-10}	410	2.4	−6.0	3.6
313	-4.23×10^{-10}	380	2.6	−5.9	3.7
intercept/cm^{-1}	1577.4				

[a] Five linear functions with a common intercept were used as model functions. For each temperature, values for W_1, $P(T)$, and $\Delta E'$ are calculated from Ω/k_{iso}. [b] For definition, see eq 1. [c] For definition, see eq 9. [d] For definition, see eq 10.

Figure 7 shows five iso-temperature correlation plots of the peak position Ω of the C═C stretch band against the rate of isomerization k_{iso} of S_1 *trans*-stilbene. Each plot consists of three points corresponding to hexane, octane, and decane. Though the number of data points are small for each plot, we see a clear tendency that each set of data points is well fitted with a straight line and that the five straight lines tend to converge to the same point at the limit $k_{iso} = 0$ (Figure 7a). In fact, we can successfully fit all of the data points by a least-suqares analysis to five straight lines with different slopes but having a common intercept at $k_{iso} = 0$ (Figure 7b). The obtained lines are shown as full lines in Figure 7. This least-squares analysis gives five slopes and one intercept as given in Table 1. The fact that the five straight lines in Figure 7 have a common intercept at $k_{iso} = 0$ strongly suggests that the peak position Ω is meaningfully correlated with the rate of isomerization k_{iso}. Note that the Ω value at the common intercept in Figure 7b corresponds to the C═C stretch frequency ω_1, which is free from the effect of the isomerization dynamics.

By using the value of the intercept, 1577.4 cm^{-1}, we can convert the observed peak position Ω to the frequency shift

TABLE 2: Shift of the Peak Position ($\Delta\Omega$) of the Olefinic C═C Stretch Raman Band of S_1 *trans*-Stilbene from the Extrapolated Value at $k_{iso} = 0$ (1577.4 cm^{-1}, See Table 1)[a]

solvent	*T*/K	$\Delta\Omega/cm^{-1}$	$10^{-12}W_1/s^{-1}$
hexane	283	−6.0	5.4
	293	−7.1	6.4
	298	−7.6	6.8
	303	−8.1	7.3
	313	−9.1	8.2
octane	283	−4.7	4.2
	293	−5.5	4.9
	298	−5.9	5.3
	303	−6.3	5.7
	313	−7.1	6.4
decane	283	−3.8	3.4
	293	−4.7	4.2
	298	−5.1	4.6
	303	−5.5	4.9
	313	−6.4	5.7

[a] Values for W_1 are calculated from $\Delta\Omega$.

$\Delta\Omega$ and then to the forward hopping rate W_1 with the use of eq 6. Note that a relation $\Delta\Omega = -0.21W_1$ is obtained from eq 6 by numerically integrating the function $G(\tau)\tau/(1+\tau^2)$ with $\tau_{1/2} = -0.35$. The values of W_1 thus obtained are given in Table 2 for three solvents and five temperatures. Table 2 tells us three important aspects of vibrational dephasing of the C═C stretch mode of S_1 *trans*-stilbene. First, the forward hopping rates have values of the order of 10^{12} s^{-1}. This fact means that the solvent fluctuation causing vibrational dephasing takes place, on an average, once in a few to ten hundred femtoseconds in the three like alkane solvents and in the temperature range 268∼338 K. Our recent theoretical simulation of the solvent-induced dynamic polarization of acetone in acetonitrile[51] is consistent with this time scale. Second, at the same temperature, W_1 increases with decreasing the size of the solvent (hexane > octane > decane). Because the mobility of the solvent is expected to decrease with increasing the solvent size, the decrease of W_1 with increasing the solvent size seems reasonable. The solvent dependent change of W_1 can also be correlated to the viscosity of the solvent which is known to increase with increasing the solvent size. The viscosity dependence of k_{iso} of S_1 *trans*-stilbene has so far been discussed in terms of the solvent dependent frequency (preexponential) factor A of the Arrhenius formula.[44,45] In the framework of the dynamic polarization model, as shown in the following, W_1 is reasonably correlated to *A*. Third, in the same solvent, W_1 increases with increasing temperature as is expected. The temperature dependence of W_1 in alkane solvents is likely to have complicated origins because of the rotational isomerism around the many C−C single bonds. This point is not discussed in the present paper.

Using the relation $\Delta\Omega = -0.21W_1$, we can convert $\Omega/k_{iso} = \Delta\Omega/k_{iso}$ to W_1/k_{iso} as given in the second column of Table 1. The experimental linear relationship between the peak position Ω and the isomerization rate k_{iso} at a fixed temperature has thus been converted to the linear relationship between W_1 and k_{iso} with the help of eqs 6 and 8. We rewrite this relationship as

$$k_{iso} = W_1 P(T) \tag{9}$$

where $P(T)$ is a temperature-dependent coefficient whose values are given in the third column of Table 1. We have already given a rationale for eq 9 in which we assume that the dynamic polarization mechanism is involved in the process of the isomerization as well (the dynamic polarization model of isomerization).[20,46] Because the rotation around C═C double bond occurs more easily if it is polarized, more frequent

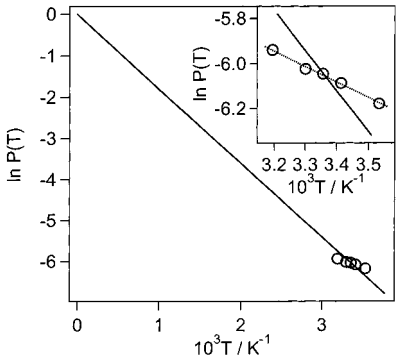

Figure 8. Values of ln $P(T)$ plotted against $1/T$. Five data points represent five different temperatures. The result of least-squares analysis is shown with a solid line. The intercept was fixed to 0 for the analysis. An expanded view for the temperature range between 283 and 313 K is shown in the inset at the upper right corner. The dotted line represents the result of least-squares analysis in which the intercept was not fixed to 0.

polarization (a larger W_1) is likely to lead to a higher isomerization rate. If $P(T) = 1$, the rate of isomerization is equal to W_1 meaning that all of the dynamic polarizations contributing vibrational dephasing are effective for the isomerization. In reality, $P(T)$ is much smaller than unity; only a small portion of dynamic polarizations (that cause vibrational dephasing) is effective for the isomerization. For example, at 293 K, only one polarization in 440 (see the third column of Table 1) is effective for the isomerization.

To consider further the physical meaning of eq 9, we compare this formula with the Arrhenius formula

$$k_{iso} = A \exp(-\Delta E/RT) \tag{10}$$

where *A* is the frequency factor, ΔE is the activation energy for the isomerization, and *R* is the gas constant. When eqs 9 and 10 are compared, the correspondence between W_1 and *A* is obvious because both of these quantities have the dimension of s^{-1}. Note, however, that *A* is often assumed to be independent of temperature but W_1 is temperature dependent. Then, $P(T)$ corresponds to the exponential factor $\exp(-\Delta E/RT)$. If we plot $\ln(P(T))$ against $1/T$ (Figure 8) and assume a relation $P(T) = \exp(-\Delta E'/RT)$, we obtain $\Delta E' = 3.6$ kcal mol^{-1}. Interestingly, this $\Delta E'$ value agrees excellently with the ΔE value, 3.5 kcal mol^{-1}, which was obtained by an iso-viscosity Arrhenius plot of the isomerization rates determined by time-resolved fluorescence spectroscopy.[52] Such an agreement was already obtained in a previous paper using the exchange model. However, in the present paper, we use more generalized dynamic polarization model and extend our studies to five different temperatures. We are now more convinced that the agreement of $\Delta E'$ and ΔE is essential and not accidental. The relation $P(T) = \exp(-\Delta E'/RT)$ can be interpreted as in the following. If the frequency $f(E)$ of the solvent fluctuation has a Boltzmann distribution such that $f(E) = \exp(-E/RT)$, where *E* represents the energy needed to cause the fluctuation, $P(T)$ gives the probability that the system has fluctuations with energy higher than $\Delta E'$. The meaning of eq 9 becomes clear with this signification of $P(T)$. The isomerization rate k_{iso} is given as the product of the forward hopping rate W_1, which represents the rate of the dynamic polarization that facilitates the rotation of the C═C bond, and the probability $P(T)$ that the solvent fluctuation is large enough for the isomerization to be complete therein.

We note that the temperature dependence of $P(T)$ shows a slight systematic deviation from the relation $P(T) = \exp(-\Delta E'/$

RT), which is seen in the inset of Figure 8. If we use another relation $P(T) = A' \exp(-\Delta E'/RT)$, we can fit the $P(T)$ values much better (see the dotted line in the inset of Figure 8) with $A' = 0.024$ and $\Delta E' = 1.4$ kcal mol^{-1}. The physical meanings of these quantities are of great interest and will be discussed in the future with more extensive data obtained in a wider temperature range.

The formulaic resemblance and the numerical agreement between eqs 9 and 10 suggests that eq 9 possesses certain generality. Though the Arrhenius formula (10) is well established and is used extensively, it itself does not tell much about the microscopic details of the chemical reaction process, as to how a chemical reaction is triggered and in what time scale it proceeds. In contrast, eq 9 tells explicitly that the isomerization reaction of S_1 *trans*-stilbene is triggered and facilitated by the solvent induced dynamic polarization of the C═C bond and that such a polarization occurs once in a few to ten hundred femtoseconds on an average in alkane solvents at room temperature, with one in about 400 of those polarizations eventually leading to the isomerization. A new perceptive view of the *trans*-stilbene photoisomerization has thus been obtained. The comprehensible nature of eq 9 makes us tempted to substantiate and establish the dynamic polarization model so that the time course of a chemical reaction can be described more lively at the molecular level. Other molecular systems suitable for testing the dynamic polarization model are now being searched for.

Acknowledgment. The authors gratefully acknowledge Dr. Chihiro Kato, Dr. Taeko Urano-Ishibashi, and Professor Mitsuo Tasumi for their collaboration in the early stage of the present work.

References and Notes

(1) Oxtoby, D. W. *Adv. Chem. Phys.* **1979**, *40*, 1.
(2) Hamaguchi, H. *Vib. Spectra Struct.* **1987**, *16*, 227.
(3) Hamaguchi, H.; Gustafson, T. L. *Annu. Rev. Phys. Chem*. **1994**, *45*, 593.
(4) Gustafson, T. L.; Roberts, D. M.; Chernoff, D. A. *J. Chem. Phys*. **1983**, *79*, 1559.
(5) Hamaguchi, H.; Kato, C.; Tasumi, M. *Chem. Phys. Lett*. **1983**, *100*, 3.
(6) Gustafson, T. L.; Roberts, D. M.; Chernoff, D. A. *J. Chem. Phys*. **1984**, *81*, 3438.
(7) Hamaguchi, H.; Urano, T.; Tasumi, M. *Chem. Phys. Lett*. **1984**, *106*, 153.
(8) Gustafson, T. L.; Chernoff, D. A.; Palmer, J. F.; Roberts, D. M. *Springer Ser. Chem. Phys.* **1984**, *38*, 266.
(9) Hamaguchi, H. *J. Mol. Struct*. **1985**, *126*, 125.
(10) Gustafson, T. L.; Chernoff, D. A.; Palmer, J. F.; Roberts, D. M. *Springer Proc. Phys.* **1985**, *4*, 15.
(11) Payne, S. A.; Hochstrasser, R. M. *J. Phys. Chem*. **1986**, *90*, 2068.
(12) Hopkins, J. B.; Rentzepis, P. M. *Chem. Phys. Lett.* **1986**, *124*, 79.
(13) Hamaguchi, H. *Chem. Phys. Lett*. **1986**, *126*, 185.
(14) Kamalov, V. F.; Koroteev, N. I.; Shkurinov, A. P.; Toleutaev, B. N. *Chem. Phys. Lett.* **1988**, *147*, 335.
(15) Hamaguchi, H. *J. Chem. Phys.* **1988**, *89*, 2587.
(16) Kamalov, V. F.; Koroteev, N. I.; Toleutaev, B. N.; Shkurinov, A. P.; Stamm, J. *J. Phys. Chem*. **1989**, *93*, 5645.
(17) Iwata, K.; Hamaguchi, H. *Chem. Phys. Lett.* **1992**, *196*, 462.
(18) Weaver, W. L.; Huston, L. A.; Iwata, K.; Gustafson, T. L. *J. Phys. Chem.* **1992**, *96*, 8956.
(19) Iwata, K.; Weaver, W. L.; Gustafson, T. L. *Chem. Phys. Lett*. **1993**, *210*, 50.
(20) Hamaguchi, H.; Iwata, K. *Chem. Phys. Lett*. **1993**, *208*, 465.
(21) Iwata, K.; Toleutaev, B.; Hamaguchi, H. *Chem. Lett*. **1993**, *9*, 1603.
(22) Hester, R. E.; Matousek, P.; Moore, J. N.; Parker, A. W.; Toner, W. T.; Towire, M. *Chem. Phys. Lett*, **1993**, *208*, 471.
(23) Qian, J.; Schultz, S. L.; Bradburn, G. R.; Jean, J. M. *J. Phys. Chem.* **1993**, *97*, 10638.
(24) Shkurinov, A. P.; Koroteev, N. I.; Jonusauskas, G.; Rulliere, C. *Chem. Phys. Lett*. **1994**, *223*, 573.
(25) Qian, J.; Schultz, S. L.; Bradburn, G. R.; Jean, J. M. *J. Lumin*. **1994**, *60/61*, 727.
(26) Okamoto, H.; Nakabayashi, T.; Tasumi, M. *J. Raman Spectrosc*. **1994**, *25*, 631.
(27) Qian, J.; Schultz, S. L.; Jean, J. M. *Chem. Phys. Lett*. **1995**, *223*, 9.
(28) Matousek, P.; Parker, A. W.; Toner, W. T.; Towire, M.; de Faria, D. L. A.; Hester, R. E.; Moore, J. N. *Chem. Phys. Lett*, **1995**, *237*, 373.
(29) Iwata, K.; Hamaguchi, H. *J. Mol. Liq*. **1995**, *65/66*, 417.
(30) Towire, M.; Matousek, P.; Parker, A. W.; Toner, W. T.; Hester, R. E. *Spectrochim. Acta A* **1995**, *51*, 2491.
(31) Oberle, J.; Abraham, E.; Ivanov, A.; Jonusauskas, G.; Rulliere, C. *J. Phys. Chem*. **1996**, *100*, 10179.
(32) Deckert, V.; Iwata, K.; Hamaguchi, H. *J. Photochem. Photobiol. A* **1996**, *102*, 35.
(33) Iwata, K.; Hamaguchi, H. *J. Phys. Chem. A* **1997**, *101*, 632.
(34) Schultz, S. L.; Qian, J.; Jean, J. M. *J. Phys. Chem. A* **1997**, *101*, 1000.
(35) Nakabayashi, T.; Okamoto, H.; Tasumi, M. *J. Phys. Chem. A* **1997**, *101*, 7189.
(36) Iwata, K.; Hamaguchi, H. *Bull. Chem. Soc. Jpn*. **1997**, *70*, 2677.
(37) Nakabayashi, T.; Okamoto, H.; Tasumi, M. *J. Phys. Chem. A* **1998**, *102*, 9686.
(38) Iwata, K.; Hamaguchi, H. *J. Raman Spectrosc*. **1998**, *29*, 915.
(39) Hamaguchi, H. *Acta Phys. Pol., A.* **1999**, *95*, 37.
(40) Nakabayashi, T.; Okamoto, H.; Tasumi, M. *Laser Chem*. **1999**, *19*, 75.
(41) Okamoto, H.; Nakabayashi, T.; Tasumi, M. *Laser Chem*. **1999**, *19*, 335.
(42) Iwata, K.; Hamaguchi, H. *Laser Chem*. **1999**, *19*, 367.
(43) Okamoto, H.; Nakabayashi, T.; Tasumi, M. *J. Raman Spectrosc*. **2000**, *31*, 305.
(44) Hochstrasser, R. M. *Pure Appl. Chem*. **1980**, *52*. 2683.
(45) Waldeck, D. H. *Chem. Rev*. **1991**, *91*, 415.
(46) Hamaguchi, H. *Mol. Phys*. **1996**, *89*, 463.
(47) Iwata, K.; Yamaguchi, S.; Hamaguchi, H. *Rev. Sci. Instrum.* **1993**, *64*, 2140.
(48) Tahara, T.; Hamaguchi, H. *Chem. Phys. Lett*. **1995**, *234*, 275.
(49) Anderson, P. W. *J. Phys. Soc. Jpn.* **1964**, *9*, 316.
(50) Shelby, R. M.; Harris, C. B.; Cornelius, P. A. *J. Chem. Phys*. **1979**, *70*, 34.
(51) Hayashi, T.; Hamaguchi, H. *Chem. Phys. Lett*. **2000**, *326*, 115.
(52) Kim, S. K.; Courtney, S. H.; Fleming, G. R. *Chem. Phys. Lett*. **1989**, *159*, 543.